

# GIAO, DFT, AIM and NBO analysis of the N–H···O intramolecular hydrogen-bond influence on the $^1J(\text{N,H})$ coupling constant in push–pull diaminoenones

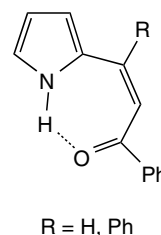
Andrei V. Afonin,\* Igor A. Ushakov, Alexander V. Vashchenko, Evgeniy V. Kondrashov and Alexander Yu. Rulev

In the series of diaminoenones, large high-frequency shifts of the  $^1\text{H}$  NMR of the N–H group in the *cis*-position relative to the carbonyl group suggests strong N–H···O intramolecular hydrogen bonding comprising a six-membered chelate ring. The N–H···O hydrogen bond causes an increase of the  $^1J(\text{N,H})$  coupling constant by 2–4 Hz and high-frequency shift of the  $^{15}\text{N}$  signal by 9–10 ppm despite of the lengthening of the relevant N–H bond. These experimental trends are substantiated by gauge-independent atomic orbital and density functional theory calculations of the shielding and coupling constants in the 3,3-bis(isopropylamino)-1-(aryl)prop-2-en-1-one (12) for conformations with the *Z*- and *E*-orientations of the carbonyl group relative to the N–H group. The effects of the N–H···O hydrogen-bond on the NMR parameters are analyzed with the atoms-in-molecules (AIM) and natural bond orbital (NBO) methods. The AIM method indicates a weakening of the N–H···O hydrogen bond as compared with that of 1,1-di(pyrrol-2-yl)-2-formylethene (13) where N–H···O hydrogen bridge establishes a seven-membered chelate ring, and the corresponding  $^1J(\text{N,H})$  coupling constant decreases. The NBO method reveals that the  $\text{LP}(\text{O}) \rightarrow \sigma^*_{\text{N-H}}$  hyperconjugative interaction is weakened on going from the six-membered chelate ring to the seven-membered one due to a more bent hydrogen bond in the former case. A dominating effect of the N–H bond rehybridization, owing to an electrostatic term in the hydrogen bonding, seems to provide an increase of the  $^1J(\text{N,H})$  value as a consequence of the N–H···O hydrogen bonding in the studied diaminoenones. Copyright © 2010 John Wiley & Sons, Ltd.

**Keywords:** NMR;  $^{15}\text{N}$  NMR; spin–spin coupling constants; N–H···O intramolecular hydrogen bond; diaminoenones; MP2; DFT and GIAO calculations; AIM and NBO analysis

## Introduction

One of the broadly used signs of hydrogen-bond formation is a pronounced high-frequency shift of the  $^1\text{H}$  NMR signal of the bridge hydrogen. Less attention was paid to how much the hydrogen bonding influences the coupling constant across the covalent bond engaged in hydrogen bonding. As the coupling constants are a source of unique structural information, a comprehensive study of this point appears to be worthwhile. It was well documented that hydrogen bonding, where the N–H covalent bond acts as a proton donor, causes a change in the relevant  $^1J(\text{N,H})$  coupling constant. Strong linear intermolecular hydrogen bonding results in a decrease of the  $^1J(\text{N,H})$  coupling constant across corresponding N–H covalent bond.<sup>[1]</sup> This trend was substantiated by *ab initio* calculations of the  $^1J(\text{N,H})$  coupling constant in hydrogen-bonded complexes.<sup>[2]</sup> The calculations also show that the decrease of the  $^1J(\text{N,H})$  coupling constant is connected with the lengthening of the N–H covalent bond.<sup>[2]</sup> The influence of intramolecular hydrogen bonding on the  $^1J(\text{N,H})$  coupling constant was less studied. The tautomeric and exchange processes complicate reliable measurement of the  $^1J(\text{N,H})$  values in many molecules with the hydrogen bonding.<sup>[3]</sup> Nevertheless, the decrease in the absolute size of the  $^1J(\text{N,H})$  coupling constant by 2–4 Hz in the *Z*-isomer of 2-(2-acylethenyl)pyrroles (Scheme 1) due to a strong N–H···O intramolecular hydrogen bond was



**Scheme 1.** Structure of the *Z*-isomer of 2-(2-acylethenyl)pyrroles.

revealed, and this experimental finding was supported by density functional theory (DFT) calculations.<sup>[4]</sup> However, the increase of the  $^1J(\text{N,H})$  coupling constant by 2–3 Hz was observed in the series of 2-substituted pyrroles with the weak N–H···N(O) intramolecular hydrogen bonds.<sup>[5]</sup>

Very recently, the series of new 3,3-bis(alkylamino)-1-(aryl)prop-2-en-1-ones was synthesized.<sup>[6]</sup> A peculiarity of the structure of push–pull diaminoenones is that an intramolecular six-membered

\* Correspondence to: Andrei V. Afonin, Institute of Chemistry, Favorski St. 1, 664033 Irkutsk, Russia. E-mail: sasha@irioch.irk.ru

Irkutsk Institute of Chemistry, 664033 Irkutsk, Russia

chelate ring with a strong N–H···O hydrogen bond is formed.<sup>[7]</sup> To gain deeper insight into the factors that determine whether an intramolecular hydrogen bond yields a decrease or increase of the  $^1J(\text{N,H})$  coupling constant, NMR spectral parameters concerning the N–H···O hydrogen bridge in the diaminoenones [ $^1J(\text{N,H})$ ,  $\delta(^1\text{H})$ ,  $\delta(^{15}\text{N})$ ] were measured. Throughout this paper, attention is mainly focused on these hydrogen-bond spectral parameters, although the complete  $^1\text{H}$ ,  $^{13}\text{C}$ ,  $^{15}\text{N}$  NMR data for the compounds studied are also included. The NMR data for the series of 1,1-di(pyrrol-2-yl)-2-acylethenes are included as well, to compare them with those of the diaminoenones, and most of them are being published for the first time (Table 1). The experimental trends are substantiated by quantum-chemical calculations. Also, with analytical purpose, the theoretical methods of Bader atoms-in-molecules (AIM) theory<sup>[8]</sup> and natural bond orbital (NBO) analysis<sup>[9]</sup> are employed.

## Results and Discussion

### Spectral data

The general formula of compounds studied in this work is shown in Scheme 2. The  $^1\text{H}$ ,  $^{13}\text{C}$  and  $^{15}\text{N}$  experimental data under consideration for the diaminoenones **1–7** and 1,1-di(pyrrol-2-yl)-2-acylethenes **8–11** are given in Table 1.

Enamino–imino tautomerism may be inherent to diaminoenones **1–7** (Scheme 3).<sup>[7]</sup> However, the values of the  $^{13}\text{C}_1$  chemical shift of the carbonyl group carbon, the  $^{13}\text{C}_2$  and  $^{13}\text{C}_3$  chemical shifts of the double bond carbons and the  $^{15}\text{N}$  chemical shifts of the amino groups nitrogen (182–184, 75–80, 159–160, –273 to –286 ppm, respectively; Table 1) unequivocally correspond to the enamino form since typical values of  $\delta(^{13}\text{C}_1)$ ,  $\delta(^{13}\text{C}_2)$ ,  $\delta(^{13}\text{C}_3)$ ,  $\delta(^{15}\text{N})$  in the diaminoenones range from 180, 90, 150, –270 to 200, 100, 160, –300 ppm, respectively.<sup>[7a]</sup> Also, a large low-frequency shift of the  $^{13}\text{C}_2$  chemical shift (~20 ppm) in the studied diaminoenones **1–7** is explained by an electron-donating effect of second amino group at the  $\text{C}_3$  carbon. Therefore, no transfer of the proton of the amino group to the oxygen of the carbonyl group takes place in the compounds **1–7**, which exist largely in the tautomeric enamino form.

The  $\delta(^1\text{H})$ ,  $\delta(^{15}\text{N})$  and  $^1J(\text{N,H})$  spectral parameters for the N–H group in the *cis*-position relative to the carbonyl group in the compounds **1–7** differ regularly from those of the N–H group in the *trans*-position. The  $^1\text{H}$  signal of the *cis*-N–H group in **1–7** is dramatically shifted to higher frequencies as compared to that of the *trans*-N–H group (11.3–11.5 vs 4.0–4.3 ppm; Table 1). This extraordinary shift occurs because of the N–H···O strong intramolecular hydrogen bond which establishes the six-membered chelate ring in the diaminoenones **1–7** (Scheme 3). Since the diaminoenones **1–7** have both the chelated N–H group in the *cis*-position to the carbonyl group and the free N–H group in the *trans*-position, these are a very convenient model to investigate the effects of N–H···O intramolecular hydrogen bonding on the NMR spectral characteristics.

The  $^{15}\text{N}$  nucleus of the *cis*-N–H group in **1–7** resonates regularly at a lower frequency with respect to that of the *trans*-N–H group (–273 to –277 vs –283 to –287 ppm; Table 1). The deshielding of the  $^{15}\text{N}$  nitrogen mainly originates from the N–H···O hydrogen bonding,<sup>[4,10]</sup> although the electronic effect of the carbonyl group may also contribute to the observed effect. One-bond  $^1J(\text{N,H})$  coupling constants across the *cis*-N–H covalent bond measured at room temperature are also larger in absolute value by 2–3 Hz

than those of the *trans*-N–H covalent bond. On lowering the temperature to  $-55^\circ\text{C}$ , the  $^1J(\text{N,H})$  coupling constants for the chelated N–H bond in **1–7** further increase by 1–2 Hz while those of the free N–H bond change to a lesser extent (Table 1). This is a somewhat surprising finding since similar N–H···O intramolecular hydrogen bonds in a series of 2-(2-acylethenyl)pyrroles cause a decrease of 2–4 Hz in the corresponding  $^1J(\text{N,H})$  value.<sup>[4]</sup> Thus, in 1,1-di(pyrrol-2-yl)-2-acylethenes **8–11**, the  $^1J(\text{N,H})$  coupling for the N–H group involved in the hydrogen bonding (*cis*-position) is smaller by 2–4 Hz than that of the free N–H group (*trans*-position; Table 1). As a result, the difference between the *cis*- $^1J(\text{N,H})$  and *trans*- $^1J(\text{N,H})$  absolute values, i.e. the parameter  $\Delta J$ , has a positive sign in the family **1–7**, while in the family **8–11** it is negative (Table 1).

In Ref. [4] it was shown that the  $\delta^1\text{H}$ ,  $\delta^{15}\text{N}$  and  $^1J(\text{N,H})$  parameters in the dipyrrolyl acylethenes depend on the solvent. Hence, the solvent effect as well as the concentration effect on these values was studied for the compound **2**.

### Solvent and concentration effects

As follows from the data in Table 2, the  $^1\text{H}$  signal of the *trans*-N–H group in **2** shifts to the higher frequencies by 1.4 and 2.0 ppm on going from  $\text{CDCl}_3$  to  $(\text{CD}_3)_2\text{CO}$  and  $(\text{CD}_3)_2\text{SO}$ , respectively, although that of the *cis*-N–H group is shifted only slightly. The *cis*- and *trans*- $^1J(\text{N,H})$  couplings change in opposite directions. While the former coupling decreases, the latter coupling increases in  $(\text{CD}_3)_2\text{CO}$  and  $(\text{CD}_3)_2\text{SO}$  as compared to  $\text{CDCl}_3$  (Table 2). The changes in the  $^{15}\text{N}$  chemical shifts are relatively small. It is worth noting only the high-frequency shift of *trans*- $\delta^{15}\text{N}$  in  $(\text{CD}_3)_2\text{SO}$  with respect to  $\text{CDCl}_3$  by 4.6 ppm. The same regularity in change of  $\delta^1\text{H}$ ,  $\delta^{15}\text{N}$  and  $^1J(\text{N,H})$  in  $\text{CDCl}_3$  and  $(\text{CD}_3)_2\text{SO}$  was discovered in dipyrrolyl acylethene **8**,<sup>[4]</sup> and the relevant parameters of **8** are also included in Table 2. It is rationalized as due to the formation of the intermolecular hydrogen bond between the free N–H group and a molecule of DMSO.<sup>[4]</sup> The same interaction with a molecule of acetone or dimethylsulfoxide (DMSO) seems to be occurring in case of molecule **2**. Notably, the  $\Delta J$  parameter in **2** demonstrates a change in sign, from positive to negative, on going from  $\text{CDCl}_3$  to  $(\text{CD}_3)_2\text{SO}$ , although it becomes more negative in the case of **8** (Table 2). The interaction with DMSO molecule leads to a decrease of the  $\Delta J$  parameter in spite of its starting value (positive or negative).

The concentration effect on  $\delta^1\text{H}$  and  $^1J(\text{N,H})$  in **2** is rather small. However, one can note some deshielding of *trans*- $^1\text{H}$  and decrease of *cis*- $^1J(\text{N,H})$  as well as the  $\Delta J$  parameter with increase of concentration (within 0.26 ppm and 0.7 Hz, respectively; Table 3). The observed trend, being like the influence of  $(\text{CD}_3)_2\text{CO}$  and  $(\text{CD}_3)_2\text{SO}$ , is probably connected with a self-association of solute molecules on increase in concentration.

### Quantum-chemical calculations

To see the effect of N–H···O intramolecular hydrogen bonding on the shielding and coupling constants, the conformations with *syn* and *anti* orientations of the carbonyl group relative to the NH(*i*-Pr) moiety of model compound **12** were taken into consideration (Scheme 4). Some geometrical parameters and calculated chemical shifts for the *syn* and *anti* conformations of **12** are shown in Table 4.

The optimized intramolecular distance  $r(\text{NH}\cdots\text{O})$  in the *syn* conformation of **12** at the MP2/6-311++G(d,p) level is only 1.77 Å

**Table 1.**  $^1\text{H}$ ,  $^{13}\text{C}$  and  $^{15}\text{N}$  NMR data for compounds **1**–**11**

Compound	Chelated N–H group		Free N–H group		$\Delta J = \frac{\text{cis-}^1J - \text{trans-}^1J}{\text{Hz}}$	C-1	C-2	C-3	$\delta^{13}\text{C}^a$ (ppm)	R <sub>1</sub> , R <sub>2</sub> , R <sub>3</sub> , pyrrole ring
	$\text{cis-}\delta^1\text{H}$	$\text{cis-}\delta^{15}\text{N}$	$\text{cis-}^1J(\text{N,H})^b$	$\text{trans-}\delta^1\text{H}$						
<b>1</b>	11.50	−276.3	90.0 (91.0) <sup>c</sup> (91.0) <sup>c</sup>	4.14	−285.5	88.2 (88.4) (88.4)	183.9	75.6	159.5	24.4, 24.8, 25.6, 32.9, 33.7 (CH <sub>2</sub> , CH <sub>2</sub> ); 49.0 (CH'); 51.0 (CH); 142.4 (C-1'); 128.0 (C-2,6'); 126.6 (C-3,5'); 129.4 (C-4)
<b>2</b>	11.49	−277.0	89.9 (91.3)	4.08	−286.6	87.3 (87.6)	183.6	75.2	159.3	21.3 (CH <sub>3</sub> ); 24.3, 24.8, 25.5, 32.8, 33.5 (CH <sub>2</sub> , CH <sub>2</sub> ); 48.8 (CH'); 50.9 (CH); 139.5 (C-1'); 128.6 (C-2,6')
<b>3</b>	11.42	−276.0	90.0 (91.6)	4.25	−286.8	88.1 (87.6)	183.0	74.7	159.3	126.4 (C-3,5'); 139.3 (C-4') 24.3, 24.8, 25.5, 29.7, 32.8, 33.5 (CH <sub>2</sub> , CH <sub>2</sub> ); 48.8 (CH'); 50.9 (CH); 55.2 (OCH <sub>3</sub> ); 134.8 (C-1'); 128.0 (C-2,6'); 113.1 (C-3,5'); 160.6 (C-4')
<b>4</b>	11.45	−275.7	90.0	4.14	−285.4	88.4	182.3	76.0	160.9	25.2, 26.1, 26.6, 33.9, 34.3 (CH <sub>2</sub> , CH <sub>2</sub> ); 49.2 (CH'); 52.4 (CH); 135.5 (C-1'); 129.2 (C-2,6')
<b>5</b>	11.36	−276.2	90.0 (91.8)	4.12	−286.1	88.4 (87.3)	183.4	80.3	159.2	128.9 (C-3,5'); 142.5 (C-4') 24.5, 24.9, 25.6, 29.8, 32.9, 33.6 (CH <sub>2</sub> , CH <sub>2</sub> ); 49.1 (CH'), 51.0 (CH); 55.6 (OCH <sub>3</sub> ); 132.9 (C-1'); 156.8 (C-2'); 111.3 (C-3'); 129.6 (C-4'); 120.4 (C-5'); 129.8 (C-6')
<b>6</b>	11.36	−273.7	90.1	4.28	−283.4	88.0	183.6	75.3	159.6	21.3 (CH <sub>3</sub> ); 23.0, 23.2 (CH <sub>3</sub> ); 41.8 (CH'), 43.9 (CH); 139.4 (C-1'); 128.6 (C-2,6'); 126.4 (C-3,5'); 139.4 (C-4')
<b>7</b>	11.44	−275.9	89.6 (90.6)	4.06	−285.6	86.6 (87.3)	183.7	75.2	160.2	10.4, 10.5 (CH <sub>3</sub> , CH <sub>3</sub> ); 20.6, 20.9 (CH <sub>3</sub> , CH <sub>3</sub> (Et)); 21.4 (CH <sub>3</sub> (Ph)), 30.0, 30.1 (CH <sub>2</sub> , CH <sub>2</sub> ); 47.6 (CH'); 49.4 (CH); 139.4 (C-1');
<b>8<sup>d</sup></b>	14.71	−220.3	93.4	8.84	−234.6	95.4	180.9	110.1	139.9	128.6 (C-2,6'); 126.5 (C-3,5'); 139.5 (C-4') 131.0 (C-2); 121.0 (C-3'); 109.8 (C-4'); 137.8 (C-5'); 133.8 (C-2'); 114.6 (C-3'); 108.1 (C-4'); 135.0 (C-5')



indicating the strong N–H···O intramolecular hydrogen bonding.<sup>[4,11]</sup> Stabilization of the *syn* conformer is evident, as it is lower in energy by as much as 8.4 kcal/mol than the *anti* conformer having no hydrogen bonding. The length of the *cis*-N–H bond in the *syn* conformation of **12** is longer by 16 mÅ than that of the *trans*-N–H bond (Table 4). Such lengthening of the *cis*-N–H bond can be attributed to the influence of the N–H···O interaction since the length of the *cis*- and *trans*-N–H bonds becomes equal in the *anti* conformation of **12** (Table 4).

The calculated <sup>1</sup>H chemical shift of the *cis*-N–H group in the *syn* conformation of **12** by means of gauge-independent atomic orbital (GIAO) is larger by 7 ppm than that of the *trans*-N–H group (10.92 vs 3.81 ppm; Table 4) reflecting the N–H···O hydrogen bonding. The difference between the calculated <sup>1</sup>H chemical shifts of the *cis*- and *trans*-N–H group matches well the experimental difference of these chemical shifts. In the *anti* conformation of **12**, the <sup>1</sup>H chemical shift of the *cis*-N–H group differs from that of the *trans*-N–H group by only 0.4 ppm (Table 4). In accordance with the computations, the <sup>15</sup>N nitrogen of the *cis*-N–H group in the *syn* conformation of **12** is deshielded by 20 ppm relative to that of the *trans*-N–H group. However, the shielding of 6.5 ppm is predicted by the calculations for the *cis*-N–H group as compared to the *trans*-N–H group in the *anti* conformation of **12** (Table 4). It implies that the N–H···O hydrogen bonding in the *syn* conformation of **12** causes the deshielding of the <sup>15</sup>N nitrogen of the *cis*-N–H group (*vide supra*), which is observed in the experiment.

A matter of special interest is the behavior of the <sup>1</sup>J(N,H) coupling constants in **12** on breaking of the N–H···O hydrogen bond. The <sup>1</sup>J(N,H) coupling constants in **12** were computed at the B3LYP/aug-cc-pVDZ level of DFT since this approach has demonstrated the close correspondence between the calculated and measured values of <sup>1</sup>J(N,H).<sup>[4,5]</sup> As calculations yield negative values of the one-bond <sup>15</sup>N–<sup>1</sup>H spin–spin coupling constant (Table 5) because of a negative value of the magnetogyric ratio γ(<sup>15</sup>N), the changes in modulus of this coupling constant are considered throughout the paper. The computed values of the <sup>1</sup>J(N,H) coupling constants for the predominant *syn* conformation of **12** are in the excellent agreement with the experimental values of **1–7** obtained at low temperature [91.4 vs 91.2 (±0.6) Hz for the chelated N–H bond and 88.5 vs 87.9 (±0.5) Hz for the free N–H bond; Tables 1 and 5]. The calculations at the DFT level show that the <sup>1</sup>J(N,H) coupling constant across the *cis*-N–H bond decreases in absolute value by 8.3 Hz, whereas that across the *trans*-N–H bond increases by 1.8 Hz on going from the *syn* to the *anti* conformation of **12** (91.4 vs 82.9 Hz and 88.5 vs 90.1 Hz; Table 5). Therefore, the N–H···O hydrogen bond in diaminoenones shows an increase of the *cis*-<sup>1</sup>J(N,H) coupling constant, indeed, in the absolute size, which is what is observed in the experiment. It should be stressed that the strengthening of the *cis*-<sup>1</sup>J(N,H) coupling in **1–7** occurs despite the lengthening of the *cis*-N–H bond (see above).

The total value of the coupling constants is known<sup>[12]</sup> to be determined by the sum of the Fermi-contact (**J<sup>FC</sup>**), the paramagnetic spin–orbital (**J<sup>PSO</sup>**), the diamagnetic spin–orbital (DSO) (**J<sup>DSO</sup>**) and the spin–dipole (**J<sup>SD</sup>**) terms (Eqn (1)).

$$\mathbf{J}^{\text{TOT}} = \mathbf{J}^{\text{FC}} + \mathbf{J}^{\text{PSO}} + \mathbf{J}^{\text{DSO}} + \mathbf{J}^{\text{SD}} \quad (1)$$

The calculations of all contributions to the one-bond <sup>1</sup>J(N,H) coupling constant reveal that the Fermi-contact contribution is the main factor that describes the influence of the N–H···O hydrogen bonding on this coupling constant in **12**. The modulus of the **J<sup>FC</sup>** term decreases by 9.3 Hz on going from the *syn* to the

*anti* conformation of **12**. At the same time, change in the **J<sup>PSO</sup>** term is of approximately 1 Hz only, and the change in the **J<sup>DSO</sup>** as well as **J<sup>SD</sup>** terms is quite negligible (Table 5). Also, the modulus of the **J<sup>FC</sup>** term of the *cis*-<sup>1</sup>J(N,H) coupling is larger by 4.1 Hz than that of the *trans*-<sup>1</sup>J(N,H) coupling in the *syn* conformation of **12**. This is a main factor to rationalize why the measured values of the *cis*-<sup>1</sup>J(N,H) coupling are larger by 2–4 Hz than those of the *trans*-<sup>1</sup>J(N,H) coupling constant in the series of diaminoenones **1–7**.

However, the opposite trend was discovered in analyzing the influence of N–H···O hydrogen bonding on <sup>1</sup>J(N,H) coupling constants in the series of 2-(2-acylethenyl)pyrroles.<sup>[4]</sup> The values of total <sup>1</sup>J(N,H) coupling constants, together with their terms for the model 1,1-di(pyrrol-2-yl)-2-formylethene **13** (Scheme 5), are also included in Table 5.

As is evident from the data of Table 5, the calculated *cis*-<sup>1</sup>J(N,H) couplings in **13** are weaker by 1–2 Hz as compared to those of *trans*-<sup>1</sup>J(N,H) depending on the conformation. Both Fermi-contact and paramagnetic spin-orbital mechanisms bring about a decrease of the *cis*-<sup>1</sup>J(N,H) absolute value in this case. A principal point in the behavior of the <sup>1</sup>J(N,H) coupling in **12** and **13** is that the **J<sup>FC</sup>** and **J<sup>PSO</sup>** terms in the latter reveal a change in the same direction providing a decrease of *cis*-**J<sup>TOT</sup>**, whereas a large increase of **J<sup>FC</sup>** for *cis*-**J<sup>TOT</sup>** in the former cancels a small decrease of **J<sup>PSO</sup>** (Table 5). Thus, the **J<sup>FC</sup>** term stipulates the different trends in the change of the measured <sup>1</sup>J(N,H) values in the diaminoenones **1–7** and 1,1-di(pyrrol-2-yl)-2-acylethenes **8–11**.

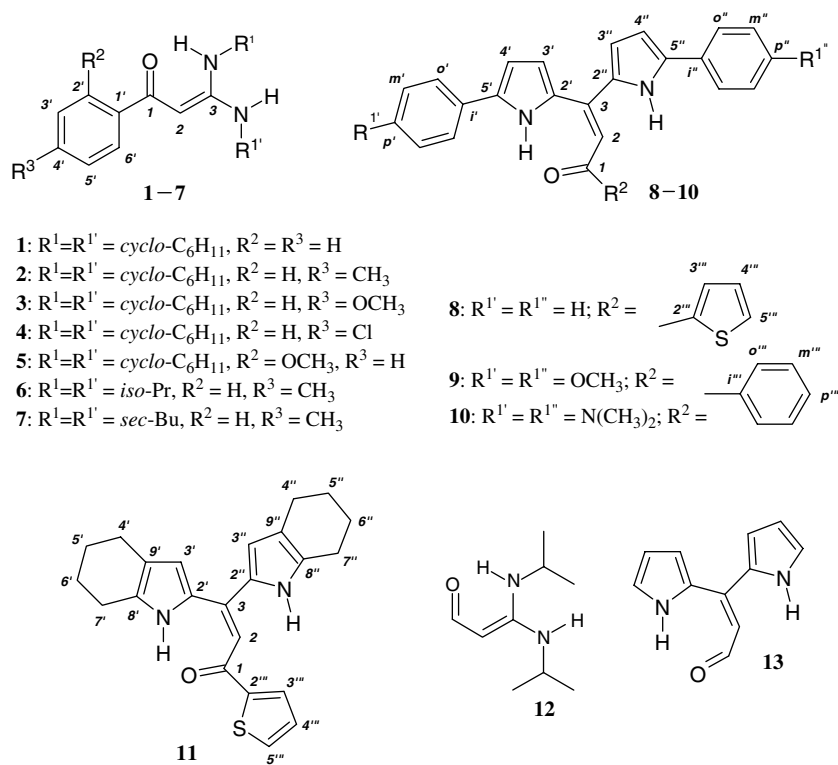
In order to elucidate the difference between the effects of the N–H···O intramolecular hydrogen bonding in the diaminoenones and dipyrrolyl acylethene, the topological parameters for hydrogen bonds in the model diaminoenone **12** and dipyrrolyl formylethene **13** obtained from AIM calculations were considered.

### AIM analysis

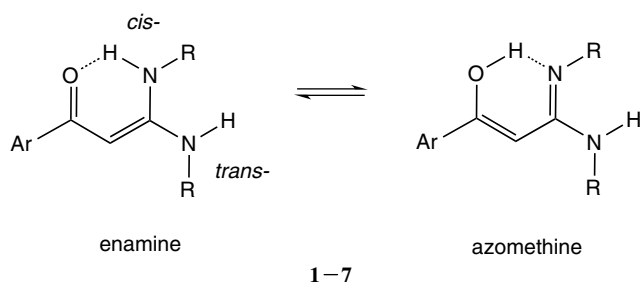
Calculations in accordance with AIM theory<sup>[8]</sup> reveal the formation of a six-membered chelate ring built up by an intramolecular N–H···O hydrogen bond in the diaminoenone **12** and a similar seven-membered chelate ring in the dipyrrolyl formylethene **13**. Topological parameters of the hydrogen bonds and chelate rings (electron density at critical points ρ; Laplacian of the electron density at critical points ∇<sup>2</sup>ρ; and the λ<sub>1</sub>, λ<sub>2</sub>, λ<sub>3</sub> eigenvalues of the Hessian matrix) as well as the energetic properties of electron density at critical points (the *G* local electron kinetic, *V* potential and *H* total energy densities) are given in Table 6.

The electron density (ρ<sup>BCP</sup><sub>H···N(O)</sub>) and other topological parameters as well as energetic characteristics of hydrogen bond critical point (BCP) (∇<sup>2</sup>ρ<sup>BCP</sup><sub>H···N(O)</sub>, λ<sub>1</sub>, λ<sub>2</sub>, λ<sub>3</sub>, *G*, *V*, *H*) of two hydrogen-bonded atoms may be treated as measures of hydrogen-bond strength.<sup>[13,14]</sup> As is evident from the data of Table 6, the ρ<sup>BCP</sup><sub>H···N(O)</sub> and ∇<sup>2</sup>ρ<sup>BCP</sup><sub>H···N(O)</sub> in the diaminoenone **12** are lower than those of dipyrrolyl formylethene **13** (3.88 × 10<sup>-2</sup> vs 4.30 × 10<sup>-2</sup> e/a<sub>0</sub><sup>3</sup> and 14.66 × 10<sup>-2</sup> vs 15.75 × 10<sup>-2</sup> e/a<sub>0</sub><sup>5</sup>, respectively). All three curvatures λ<sub>1</sub>, λ<sub>2</sub>, λ<sub>3</sub> are also smaller in the former molecule (Table 6). Finally, the *G*, *V* and *H* local energetic characteristics of BCP in **12** reduce in the absolute value as compared to those of **13** (3.69 × 10<sup>-2</sup>, -3.71 × 10<sup>-2</sup> and -0.02 × 10<sup>-2</sup> vs 4.12 × 10<sup>-2</sup>, -4.31 × 10<sup>-2</sup> and -0.19 × 10<sup>-2</sup> kJ/mol × a<sub>0</sub><sup>3</sup>, respectively; Table 6).

The listed topological parameters and energetic characteristics have been shown<sup>[14]</sup> to be connected with the intermolecular distances of the interacting atoms in the hydrogen-bonded complexes, the parameters becoming smaller as the distance



Scheme 2. Compounds studied.



Scheme 3. Possible enamine–imine tautomerism in diaminoenones 1–7.

increases. It allows one to suppose that a similar regularity takes place in the case of intramolecular interactions, and the  $\text{N-H}\cdots\text{O}$  intramolecular hydrogen bond is weakened on going from the dipyrrolyl formylethene **13** to the diaminoenone **12**. The weakening of the  $\text{N-H}\cdots\text{O}$  hydrogen bond in **12** with respect to that in **13** reflects the elongation of the  $\text{H}\cdots\text{O}$  intramolecular distance from 1.68 Å<sup>[4]</sup> in the latter molecule to 1.78 Å in the former molecule. Besides, the ratios  $|\lambda_1 + \lambda_2|/\lambda_3$  and  $|V|/G$  in **13** show some increase relative to those of **12** (0.476 vs 0.446 and 1.045 vs 1.007; Table 6) indicating an enhancement of the stabilizing effect of the electric field over the repulsive, closed-shells interaction in hydrogen bonding.<sup>[14]</sup>

One of the essential reasons for the weakening of the hydrogen bridge in diaminoenone **12** in comparison to that in dipyrrolyl formylethene **13** is the more strained nature of the six-membered chelate ring in the former with respect to the seven-membered chelate ring in the latter. The bond angle  $\theta$  at the bridge hydrogen (Scheme 6) in the diaminoenone **12**, corresponding to the equilibrium geometry, is 142.5° (Table 4), while that of **13** increases to 152.7°.<sup>[4]</sup>

From a topological parameter viewpoint, one can see a significant increase of both the  $\rho^{\text{RCP}}$  electron density and  $\nabla^2\rho^{\text{RCP}}$  Laplacian of the electron density at the critical point of the chelate ring on going from the seven-membered chelate ring in **13** to the six-membered chelate ring in **12** ( $0.77 \times 10^{-2}$  vs  $1.65 \times 10^{-2} e/a_0^3$  and  $4.98 \times 10^{-2}$  vs  $11.29 \times 10^{-2} e/a_0^5$ , respectively; Table 6), showing the more linear character of the hydrogen bond in the former molecule.

Thus, an analysis of the topological and geometrical parameters of the  $\text{N-H}\cdots\text{O}$  hydrogen bond in the molecules **12** and **13** suggests that the more bent hydrogen bond in the case of the six-membered chelate ring of **12** is weaker. As a result of this weakening, the effect of the  $\text{N-H}\cdots\text{O}$  hydrogen bond on the  $^1J(\text{N,H})$  coupling constant changes the direction (increase in the former molecules and decrease in the latter molecules). To gain more unambiguous interpretation of the discussed phenomena, the NBO method of Weinhold *et al.*<sup>[9]</sup> was employed.

### NBO analysis

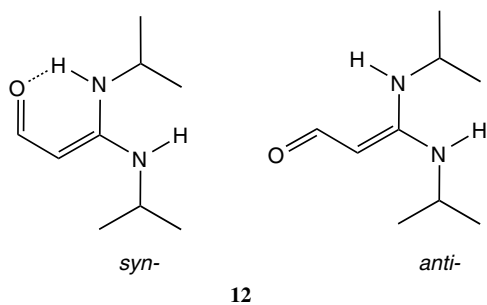
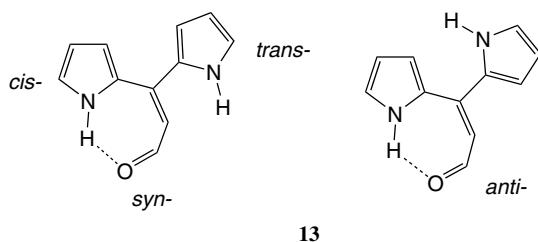
The relevant parameters taken from the NBO analysis are presented in Table 7. As shown by the NBO analysis, there are a strong hyperconjugative interactions between both oxygen lone pairs and the antibonding orbital of the  $\text{N-H}$  bond,  $\text{LP}_1(\text{O}) \rightarrow \sigma^*_{\text{N-H}}$  and  $\text{LP}_2(\text{O}) \rightarrow \sigma^*_{\text{N-H}}$ , in the molecules **12** and **13**, providing a charge transfer from the former moieties to the latter moiety through the intramolecular  $\text{N-H}\cdots\text{O}$  hydrogen bond. The  $\text{LP}_1(\text{O}) \rightarrow \sigma^*_{\text{N-H}}$  and  $\text{LP}_2(\text{O}) \rightarrow \sigma^*_{\text{N-H}}$  interactions in the pyrrole **13** are noticeably stronger than those in diaminoenone **12** (7.46 vs 4.66 and 19.59 vs 16.06 kcal/mol; Table 7), yielding the total intensification of the  $\text{LP}_{1,2}(\text{O}) \rightarrow \sigma^*_{\text{N-H}}$  interaction in **13** by 6.3 kcal/mol. The reinforcement of the  $\text{LP}_{1,2}(\text{O}) \rightarrow \sigma^*_{\text{N-H}}$  interaction in **13** can be rationalized by the more linear  $\text{N-H}\cdots\text{O}$

**Table 2.**  $^1\text{H}$ , and  $^{15}\text{N}$  NMR data for compounds **2** and **8** in the different solvents

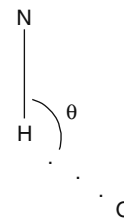
Compound	Solvent	$\delta$ (ppm)				$J$ (Hz)		$\Delta J$
		<i>cis</i> - $\delta^1\text{H}$	<i>cis</i> - $\delta^{15}\text{N}$	<i>trans</i> - $\delta^1\text{H}$	<i>trans</i> - $\delta^{15}\text{N}$	<i>cis</i> - $^1J(\text{N,H})$	<i>trans</i> - $^1J(\text{N,H})$	
<b>2</b>	$\text{CDCl}_3$	11.49	−277.0	4.08	−286.6	89.9	87.3	2.6
	$(\text{CD}_3)_2\text{CO}$	11.78	−277.4	5.45	−285.3	89.2	88.8	0.4
	$(\text{CD}_3)_2\text{SO}$	11.46 (−0.03) <sup>a</sup>	−275.8 (1.2)	6.10 (2.02)	−282.0 (4.6)	87.8 (−2.1)	89.4 (2.1)	−1.6
<b>8</b> <sup>b</sup>	$\text{CDCl}_3$	14.71	−220.3	8.84	−234.6	93.4	95.4	−2.0
	$(\text{CD}_3)_2\text{SO}$	14.46 (−0.25) <sup>a</sup>	−222.0 (−1.7)	11.86 (3.02)	−229.8 (5.8)	92.3 (−1.1)	96.8 (1.4)	−4.5

<sup>a</sup> The differences between spectral parameters in  $(\text{CD}_3)_2\text{SO}$  and  $\text{CDCl}_3$  are given in parentheses.<sup>b</sup> The data were taken from Ref. [4].**Table 3.** Effect of solvent concentration on the  $^1\text{H}$  chemical shift and  $^1J(\text{N,H})$  coupling constant in 3,3-bis(cyclohexylamino)-1-(4-methylphenyl)prop-2-en-1-one **2** in  $\text{CDCl}_3$ 

Solvent concentration (M)	$\delta$ (ppm)		$J$ (Hz)		$\Delta J$
	<i>cis</i> - $\delta^1\text{H}$	<i>trans</i> - $\delta^1\text{H}$	<i>cis</i> - $^1J(\text{N,H})$	<i>trans</i> - $^1J(\text{N,H})$	
0.013	11.49	4.08	89.9	87.3	2.6
0.026	11.53	4.11	89.7	87.4	2.3
0.052	11.53	4.13	89.5	87.4	2.1
0.105	11.53	4.16	89.3	87.3	2.0
0.210	11.51	4.22	89.3	87.3	2.0
0.420	11.50	4.34	89.2	87.3	1.9

**12****Scheme 4.** The conformations studied for 3,3-bis(isopropylamino)-1-prop-2-en-1-one (**12**).**13****Scheme 5.** The conformations studied for 1,1-di(pyrrole-2-yl)-2-formylethene (**13**).

intramolecular hydrogen bonding in case of the seven-membered chelate ring. As a consequence of the  $\text{LP}_{1,2}(\text{O}) \rightarrow \sigma^*_{\text{N-H}}$  interaction, the  $\sigma^*_{\text{N-H}}$  occupation number for the chelated N–H bond in **12**, **13** becomes greater than that of the free N–H bond. A more intensive  $\text{LP}_{1,2}(\text{O}) \rightarrow \sigma^*_{\text{N-H}}$  interaction in **13** ensures

**Scheme 6.** Hydrogen-bond angle.

a larger difference between the  $\sigma^*_{\text{N-H}}$  occupation numbers for the chelated and free N–H bonds in comparison with that of **12** (0.033 and 0.047 *e*, respectively; Table 7). An increase of the  $\sigma^*_{\text{N-H}}$  occupation numbers for the *cis*-N–H bond should result in the lengthening of this bond as well as weakening of the corresponding  $^1J(\text{N,H})$  coupling.<sup>[15]</sup>

As hydrogen bonding involves electrostatic and charge transfer interactions,<sup>[16]</sup> it is necessary to allow for a rehybridization of the N–H bond, due to the electrostatic term, to lead to a change of the bond length and one-bond coupling constant in a direction opposite to that of the charge transfer interaction.<sup>[12b,17]</sup> As evident from data in Table 7, the percentage of nitrogen *s*-character of the *cis*-N–H bond is higher in **12** and **13** than that of the *trans*-N–H bond (28.1 vs 26.3 and 31.0 vs 27.5%). Obviously, the electrostatic interaction in the seven-membered chelate ring in **13** is stronger once again than that of the six-membered chelate ring in **12** since the nitrogen *s*-character increases by *ca* 4% on going from the *cis*-N–H bond to the *trans*-N–H bond in **13**, while an increase of only 2% is observed for the nitrogen *s*-character of the *cis*-N–H bond as compared to that of the *trans*-N–H bond in **12**. A change in the *s*-character percentage of the N–H bond affects the relevant shielding and coupling constants. From a theoretical viewpoint, an increased *s*-character of a bond to nitrogen yields a high-frequency shift of the corresponding  $^{15}\text{N}$  NMR signal owing to an increase in the negative local paramagnetic term of the total nuclear shielding.<sup>[18]</sup> The *cis*- $^{15}\text{N}$  nitrogen in the diaminoenones **1–7** shows a high-frequency shift of 10–11 ppm, indeed, and this effect is substantiated by the GIAO calculations (see above). Also, since there is a linear relationship between the one-bond  $^1J(\text{N,H})$  coupling constants and the nitrogen *s*-character percentage of the N–H bond, the absolute value of  $^1J(\text{N,H})$  increases as the percent *s*-character of the N–H bond at the nitrogen atom increases.<sup>[12b,17]</sup> It corresponds to the observed increase of the *cis*- $^1J(\text{N,H})$  coupling constant in **1–7** relative to that of the *trans*- $^1J(\text{N,H})$  coupling constant.

**Table 4.** Selected geometrical parameters and calculated chemical shifts for the *syn* and *anti* conformers of **12**

Conformer	Hydrogen bond angle ( $\theta$ )	R ( $\text{\AA}$ )			$\delta$ (ppm)			
		H $\cdots$ O	<i>cis</i> -N-H	<i>trans</i> -N-H	<i>cis</i> -N- $^1\text{H}$	<i>trans</i> -N- $^1\text{H}$	<i>cis</i> - $^{15}\text{N}$ -H	<i>trans</i> - $^{15}\text{N}$ -H
<i>Syn</i>	142.5	1.775	1.030	1.013	10.92	3.81	-279.2	-299.2
<i>anti</i>	-	3.727	1.014	1.014	2.90	2.53	-286.8	-280.3

**Table 5.** Calculated coupling constants for the *syn* and *anti* conformers of **12** and **13**

Compound		J (Hz)									
Conformer		<i>cis</i> - $^1\text{J}(\text{N},\text{H})$					<i>trans</i> - $^1\text{J}(\text{N},\text{H})$				
		$\text{J}^{\text{TOT}}$	$\text{J}^{\text{FC}}$	$\text{J}^{\text{PSO}}$	$\text{J}^{\text{DSO}}$	$\text{J}^{\text{SD}}$	$\text{J}^{\text{TOT}}$	$\text{J}^{\text{FC}}$	$\text{J}^{\text{PSO}}$	$\text{J}^{\text{DSO}}$	$\text{J}^{\text{SD}}$
<b>12</b>	<i>Syn</i>	-91.4	-89.8	-1.1	-0.6	0	-88.5	-85.6	-2.2	-0.6	-0.1
	<i>anti</i>	-82.9	-80.4	-2.1	-0.5	0	-90.1	-87.3	-2.2	-0.5	-0.1
<b>13</b> <sup>a</sup>	<i>syn</i>	-95.1	-93.8	-0.7	-0.6	0	-96.3	-93.9	-1.8	-0.5	-0.1
	<i>anti</i>	-94.9	-93.7	-0.7	-0.6	0	-96.9	-94.6	-1.7	-0.6	0

<sup>a</sup> Taken from Ref. [4]. As the  $^{14}\text{N}$ - $^1\text{H}$  coupling constants were erroneously reported in the previous paper,<sup>[4]</sup> they are converted to the corresponding  $^{15}\text{N}$ -based values using the equation  $J(^{15}\text{N}, \text{H}) = -1.4027 J(^{14}\text{N}, \text{H})$  where the coefficient is the ratio of magnetogyric ratios  $\gamma(^{15}\text{N})/\gamma(^{14}\text{N})$ . The *syn* and *anti* conformations correspond the rotation of the *trans* pyrrole ring (Scheme 5).

The competition between the rehybridization and hyperconjugation effects on the  $^1\text{J}(\text{N},\text{H})$  coupling constant, operating in opposite directions, may result in a decrease in the  $^1\text{J}(\text{N},\text{H})$  absolute magnitude or an increase in the hydrogen bonding. Both electrostatic and charge transfer interactions are stronger in the case of the seven-membered chelate ring in comparison to the six-membered chelate ring (compounds **12** and **13**, respectively). Nevertheless, based on the experimentally observed and theoretically predicted trends in the change of the  $^1\text{J}(\text{N},\text{H})$  values for the dipyrrolyl formyl(acyl)ethenes and diaminoenones, one can guess that the strong  $\text{LP}(\text{O}) \rightarrow \sigma^*_{\text{N-H}}$  interaction in **13** prevails over the rehybridization effect and that the  $^1\text{J}(\text{N},\text{H})$  coupling constant decreases as a result of the stronger  $\text{N-H}\cdots\text{O}$  intramolecular hydrogen bonding. However, a less important  $\text{LP}(\text{O}) \rightarrow \sigma^*_{\text{N-H}}$  interaction in **12** is smaller compared to the rehybridization effect and an increase of the  $^1\text{J}(\text{N},\text{H})$  coupling constant is exhibited as a consequence of the more bent  $\text{N-H}\cdots\text{O}$  intramolecular hydrogen bond for the six-membered chelate ring. As expected, the term most sensitive to the rehybridization and hyperconjugation effects turns out to be the Fermi-contact ( $\text{J}^{\text{FC}}$ ) term of the total  $^1\text{J}(\text{N},\text{H})$  spin-spin coupling constant (see above).

## Conclusion

An experimental and theoretical investigation of the influence of  $\text{N-H}\cdots\text{O}$  intramolecular hydrogen bonding on the one-bond  $^1\text{J}(\text{N},\text{H})$  spin-spin coupling constant in push-pull diaminoenones finds no direct correlation between the  $\text{N-H}$  bond length and the  $^1\text{J}(\text{N},\text{H})$  value. Lengthening of the  $\text{N-H}$  covalent bond in hydrogen bonding may be accompanied by an increase in the  $^1\text{J}(\text{N},\text{H})$  coupling constant in absolute size rather than its decrease. This is the case when the rehybridization effect of the  $\text{N-H}$  bond, due to the electrostatic term of hydrogen bonding, predominates over the hyperconjugation effect. The factor leading to a weakening of the hyperconjugation between the oxygen atom lone pairs and antibonding orbital of the  $\text{N-H}$  bond is the bent geometry of

the hydrogen bond. An increase of the absolute value of  $^1\text{J}(\text{N},\text{H})$  should be expected for a bent hydrogen bond, while a decrease of the  $^1\text{J}(\text{N},\text{H})$  coupling constant is expected on the formation of a more linear hydrogen bond. The observed effect depends on the solvent. In a basic solvent such as DMSO, a positive effect of the intramolecular hydrogen bonding on the  $^1\text{J}(\text{N},\text{H})$  coupling constant may be replaced by a negative effect since a solvent molecule can form a competitive intermolecular hydrogen bonding.

## Experimental and Computational Details

### Spectra

NMR spectra were recorded in  $\text{CDCl}_3$  at 303 K on a Bruker AVANCE 400 spectrometer ( $^1\text{H}$ , 400.16 MHz;  $^{13}\text{C}$ , 101.61 MHz;  $^{15}\text{N}$ , 40.55 MHz) equipped with a 5-mm Z-gradient inversion probehead and XWIN-NMR 3.5 software package running on Windows XP. The  $^1\text{H}$  and  $^{13}\text{C}$  chemical shifts were referenced to internal TMS.

The application of the homonuclear two-dimensional (2D) COSY and NOESY as well as heteronuclear 2D HSQC and HMBC methods allowed the assignment of the  $^1\text{H}$  and  $^{13}\text{C}$  signals in compounds **1–11**. To minimize the effect of the intermolecular hydrogen bonding, the values of the one-bond  $^{15}\text{N}$ - $^1\text{H}$  coupling constants were measured in a 2D [ $^1\text{H}$ - $^{15}\text{N}$ ] gHSQC experiment.<sup>[19]</sup> The values of the  $^1\text{J}(\text{N},\text{H})$  coupling constant were determined from the one-dimensional (1D) traces of the 2D [ $^1\text{H}$ - $^{15}\text{N}$ ] HSQC maps. The measurement of the  $^1\text{J}(\text{N},\text{H})$  values were carried out at +25 and -55 °C. A standard Bruker pulse program hsqcgpqh without GARP decoupling during acquisition was used. The acquisition conditions consisted of  $4\text{K} \times 256$  datapoints without zero-filling taken over sweep widths of 1.0 ( $^1\text{H}$ ,  $F_2$ ), 100 ( $^{15}\text{N}$ ,  $F_1$ ) ppm. The digital resolution in the 1D traces from  $F_2$  projection was 0.1 Hz per point, and the uncertainty in the  $^1\text{J}(\text{N},\text{H})$  coupling constants was 0.1 Hz. The values of the  $\delta(^{15}\text{N})$  were measured through a 2D [ $^1\text{H}$ - $^{15}\text{N}$ ] HMBC experiment.<sup>[20]</sup> The  $^{15}\text{N}$  chemical shifts were referenced to  $\text{CH}_3\text{NO}_2$  used as an external standard in a capillary.

**Table 6.** Topological parameters and energetic characteristics of the intramolecular hydrogen bonds and chelate rings in the compounds **12** and **13**<sup>a</sup>

Compound	NH···O hydrogen BCP		Ring critical point		Eigenvalues of the Hessian matrix				Energetic properties of electron density at BCP			
	$\rho^{\text{BCP}}_{\text{O}\cdots\text{H}}$ $\times 10^2$	$\nabla^2\rho^{\text{BCP}}_{\text{O}\cdots\text{H}}$ $\times 10^2$	$\rho_{\text{RCP}}$ $\times 10^2$	$\nabla^2\rho_{\text{RCP}}$ $\times 10^2$	$\lambda_1$ $\times 10^2$	$\lambda_2$ $\times 10^2$	$\lambda_3$ $\times 10^2$	$ \lambda_1 + \lambda_2 /\lambda_3$	$G \times 10^2$	$V \times 10^2$	$H \times 10^2$	$ V /G$
<b>12</b>	3.88	14.66	1.65	11.29	−6.01	−5.81	26.49	0.446	3.69	−3.71	−0.02	1.007
<b>13</b>	4.30	15.75	0.77	4.98	−7.33	−6.99	30.08	0.476	4.12	−4.31	−0.19	1.045

<sup>a</sup> The  $\rho$  and  $\nabla^2\rho$ ,  $\lambda_1, \lambda_2, \lambda_3$  values are given in  $e/a_0^3$  and  $e/a_0^5$ , respectively; the  $G, V, H$  are given in kJoule per mol  $\times a_0^3$ .

**Table 7.** Energy of the NBO hyperconjugative interactions, NBO nitrogen *s*-character percentage of the N–H bonds<sup>a</sup> and occupancy of the antibonding  $\sigma^*_{\text{N-H}}$  orbitals for the compounds **12** and **13**

Compound	Energy stabilization (kcal/mol)		Occupancy ( <i>e</i> )		<i>s</i> -character of natural bond orbital (%)	
	LP <sub>1</sub> (O) → $\sigma^*_{\text{N-H}}$	LP <sub>2</sub> (O) → $\sigma^*_{\text{N-H}}$	<i>cis</i> - $\sigma^*_{\text{N-H}}$	<i>trans</i> - $\sigma^*_{\text{N-H}}$	<i>cis</i> -N–H	<i>trans</i> -N–H
<b>12</b>	4.66	16.06	0.03346	0.01935	28.07	26.25
<b>13</b>	7.46	19.59	0.04668	0.01521	30.95	27.53

<sup>a</sup> In all cases, the *H s*-character ranges from 99.93 to 99.96%.

The concentrations of solute molecules were within 0.01–0.05 M.

## Calculations

The geometries for all structures presented here were calculated at the MP2 level of theory<sup>[21]</sup> without symmetry constraints by using the Gaussian 03 W program package.<sup>[22]</sup> The triple split-valence 6-311G++(d,p) basis set of Pople, which included a set of diffuse functions as well as d-type polarization functions on all non-hydrogen atoms and p-type polarization functions on hydrogen atoms, was adopted in the calculations.<sup>[23]</sup> The energy minima with respect to the nuclear coordinates were obtained by the simultaneous relaxation of all the geometrical parameters of the molecules using the gradient method of Pulay.<sup>[24]</sup> Frequency calculations at equilibrium geometries yielded no imaginary values, indicating that the geometries obtained corresponded to energy minima.

The proton and nitrogen magnetic shielding constants were computed via the GIAO method<sup>[25]</sup> in the DFT framework. The effect of electron correlation on DFT calculations was taken into account by Becke's three-parameter hybrid exchange function<sup>[26]</sup> and correlation functional by Lee, Parr and Yang (B3LYP).<sup>[27]</sup> The proton and nitrogen shielding constants calculations were carried out for the MP2/6-311G++(d,p) optimized geometries using Dunning's correlation consistent basis set of double zeta quality augmented with standard diffuse functions (aug-cc-pVDZ).<sup>[28]</sup> Absolute isotropic shielding constants were also calculated for the reference materials TMS and CH<sub>3</sub>NO<sub>2</sub>, and the values of proton and nitrogen chemical shifts were obtained as the difference between the proton and nitrogen shielding constants for the investigated compounds and that for TMS and CH<sub>3</sub>NO<sub>2</sub>, respectively.

The total value of the coupling constant was determined as the sum of the Fermi-contact, paramagnetic spin–orbital, DSO and spin–dipole contributions. They were computed for the MP2/6-311G++(d,p) optimized geometries using the aug-cc-pVDZ basis set with the B3LYP density functional for all types of coupling.

The three second-order terms (the Fermi-contact, paramagnetic spin–orbital and spin–dipole) were calculated using the coupled-perturbed Kohn–Sham (CP-KS) approach.<sup>[29]</sup> The first-order DSO term was calculated as the mean value of the DSO operator in the unperturbed reference state.<sup>[29]</sup>

AIM calculations of topological parameters at the B3LYP/6-311++G(d,p) level were performed as implemented in the Gaussian 03 program. NBO characteristics (energy of the hyperconjugative interactions, nitrogen and hydrogen *s*-character percentage of the N–H bonds, occupancy of lone pair and antibonding  $\sigma^*_{\text{N-H}}$  orbitals) were obtained through the NBO program<sup>[30]</sup> at MP2/6-311++G(d,p) level.

## Synthesis of 1–7

The syntheses of 3,3-bis(alkylamino)-1-(aryl)prop-2-en-1-ones **1–6** have been previously described.<sup>[6]</sup> Diaminoenone **7** was synthesized in the same way.

### 1-(4-Methylphenyl)-3,3-bis[(1-methylpropyl)amino]prop-2-en-1-one (**7**)

A mixture of the corresponding bromostyrene (1 mmol) and *sec*-butylamine (10 mmol) was refluxed in dioxane for 32 h. Then the solvent was evaporated *in vacuo*, a solution of concentrated HCl (5 ml) was added and the mixture was heated at 70 °C for 3 h and then extracted by CHCl<sub>3</sub>. The target enone **7** was isolated by column chromatography (silica gel, CHCl<sub>3</sub>: MeOH = 19:1). Yield: 228 mg (79%); yellow solid; m.p. 143–145 °C. <sup>1</sup>H and <sup>13</sup>C NMR (Table 1). MS (EI) *m/z* (relative intensity): 288 (31) [M<sup>+</sup>], 231 (10), 160 (35), 147 (16), 119 (100), 91 (50), 72 (90). C<sub>18</sub>H<sub>28</sub>N<sub>2</sub>O (288.428): calcd. C 74.96, H 9.78, N 9.71; found C 74.79, H 9.75, N 9.84.

## Acknowledgement

This study was supported by the Russian Foundation for Basic Research (Grant Nos 08-03-00736-a, RFBR-DFG 07-03-91562-NNO\_a and 08-03-00067-a).

## References

- [1] (a) A. J. Dingley, J. E. Masse, R. D. Peterson, M. Barfield, J. Feigon, S. Grzesiek, *J. Am. Chem. Soc.* **1999**, *121*, 6019; (b) E. M. B. Janke, A. Dunger, H.-H. Limbach, K. Weisz, *Magn. Reson. Chem.* **2001**, *39*, S177; (c) R. Ishikawa, C. Kojima, A. Ono, M. Kainosho, *Magn. Reson. Chem.* **2001**, *39*, S159.
- [2] (a) J. E. Del Bene, J. Elguero, *J. Phys. Chem. A* **2006**, *110*, 7496; (b) J. E. Del Bene, J. Elguero, *J. Am. Chem. Soc.* **2004**, *126*, 15624.
- [3] I. Alkorta, J. Elguero, G. S. Denisov, *Magn. Reson. Chem.* **2008**, *46*, 599.
- [4] A. V. Afonin, I. A. Ushakov, L. N. Sobenina, Z. V. Stepanova, O. V. Petrova, B. A. Trofimov, *Magn. Reson. Chem.* **2006**, *44*, 59.
- [5] (a) A. V. Afonin, I. A. Ushakov, A. I. Mikhaleva, B. A. Trofimov, *Magn. Reson. Chem.* **2007**, *45*, 220; (b) A. V. Afonin, A. V. Vashchenko, I. A. Ushakov, N. V. Zorina, E. Yu. Schmidt, *Magn. Reson. Chem.* **2008**, *46*, 441.
- [6] A. Yu. Rulev, V. M. Muzalevskiy, E. V. Kondrashov, I. A. Ushakov, A. V. Shastin, E. S. Balenkova, G. Haufe, V. G. Nenajdenko, *Eur. J. Org. Chem.* **2010**, 300.
- [7] (a) J. L. Chiara, A. Gomez-Sanchez, in *The Chemistry of Enamines*, (Eds: Z. Rappoport), Wiley & Sons: New York, **1994**, Chapter 5, p 279; (b) A. Perona, D. Sanz, R. M. Claramunt, J. Elguero, *Magn. Reson. Chem.* **2008**, *46*, 930.
- [8] R. F. W. Bader, *Atoms in Molecules. A Quantum Theory*, Oxford University Press: New York, **1990**.
- [9] (a) A. E. Reed, L. A. Curtiss, F. Weinhold, *Chem. Rev.* **1988**, *88*, 899; (b) F. Weinhold, in *Encyclopedia of Computational Chemistry*, vol. 3, (Eds: P. V. R. Schleyer), Wiley: New York, **1998**, p 1792.
- [10] M. Weychert, J. Klimkiewicz, I. Wawer, B. Piekarska-Bartoszewicz, A. Temeriuć, *Magn. Reson. Chem.* **1998**, *36*, 727.
- [11] (a) N. N. Chipanina, V. K. Turchaninov, I. I. Vorontsov, M. Yu. Antipin, Z. V. Stepanova, L. N. Sobenina, A. I. Mikhaleva, B. A. Trofimov, *Russ. Chem. Bull.* **2002**, *51*, 107; (b) Z. V. Stepanova, L. N. Sobenina, A. I. Mikhaleva, I. A. Ushakov, V. N. Elokhina, I. I. Vorontsov, M. Yu. Antipin, B. A. Trofimov, *Zh. Org. Khim.* **2003**, *39*, 1705.
- [12] (a) N. F. Ramsey, *Phys. Rev.* **1953**, *91*, 303; (b) R. H. Contreras, V. Barone, J. C. Facelli, J. E. Peralta, *Annu. Rep. NMR Spectrosc.* **2003**, *51*, 167.
- [13] (a) S. J. Grabowski, *Chem. Phys. Lett.* **2001**, *338*, 361; (b) S. Wojtulewski, S. J. Grabowski, *Chem. Phys. Lett.* **2003**, *378*, 388; (c) T.-H. Tang, E. Deretey, S. J. Knak Jensen, G. Csizmadia, *Eur. Phys. J. D* **2006**, *37*, 217.
- [14] (a) E. Espinosa, I. Alkorta, J. Elguero, E. Molins, *J. Chem. Phys.* **2002**, *117*, 5529; (b) I. Mata, E. Molins, I. Alkorta, E. Espinosa, *J. Phys. Chem. A* **2007**, *111*, 6425; (c) I. Mata, I. Alkorta, E. Molins, E. Espinosa, *Chem. Eur. J.* **2010**, *16*, 2442.
- [15] (a) C. Vizioli, M. C. Ruiz de Azua, C. G. Giribet, R. H. Contreras, L. Turi, J. J. Dannenberg, I. D. Rae, J. A. Weingold, M. Malagoli, R. Zanasi, P. Lazzarotti, *J. Phys. Chem.* **1994**, *98*, 8858; (b) A. J. Dingley, J. E. Masse, R. D. Peterson, M. Barfield, J. Feigon, S. Grzesiek, *J. Am. Chem. Soc.* **1999**, *121*, 6019; (c) R. H. Contreras, J. E. Peralta, C. G. Giribet, M. C. Ruiz de Azua, J. C. Facelli, *Annu. Rep. NMR Spectrosc.* **2000**, *41*, 55; (d) E. M. B. Janke, A. Dunger, H.-H. Limbach, K. Weisz, *Magn. Reson. Chem.* **2001**, *39*, S177; (e) G. L. Sosa, N. M. Peruchena, R. H. Contreras, E. A. Castro, *J. Mol. Struct.* **2002**, *577*, 219.
- [16] (a) K. Kitaura, K. Morokuma, *Int. J. Quantum Chem.* **1976**, *10*, 325; (b) K. Morokuma, K. Kitaura, Energy decomposition analysis of molecular interactions. in *Chemical Applications of Atomic and Molecular Electrostatic Potentials*, (Eds: P. Politzer, D. G. Truhlar), Plenum: New York, **1981**, p 215.
- [17] R. H. Contreras, J. E. Peralta, C. G. Giribet, M. C. Ruiz de Azua, J. C. Facelli, *Ann. Rep. NMR Spectrosc.* **2000**, *41*, 55.
- [18] C. G. Levy, R. L. Lichter, *Nitrogen-15 NMR Magnetic Resonance Spectroscopy*, Wiley-Interscience: New York, **1979**.
- [19] G. Bodenhausen, D. Ruben, *J. Chem. Phys. Lett.* **1980**, *69*, 185.
- [20] A. Bax, M. F. Summers, *J. Am. Chem. Soc.* **1986**, *108*, 2093.
- [21] C. Møller, M. S. Plesset, *Phys. Rev.* **1934**, *46*, 618.
- [22] M. J. Frisch, G. W. Trucks, H. B. Schlegel, G. E. Scuseria, M. A. Robb, J. R. Cheeseman, J. A. Montgomery, T. Vreven, K. N. Kudin, J. C. Burant, J. M. Millam, S. Iyengar, J. Tomasi, V. Barone, B. Mennucci, M. Cossi, G. Scalmani, N. Rega, G. A. Petersson, H. Nakatsuji, M. Hada, M. Ehara, K. Toyota, R. Fukuda, J. Nasegawa, M. Ishida, T. Nakajima, Y. Honda, O. Kitao, H. Nakai, M. Klene, X. Li, J. E. Knox, H. P. Hratchian, J. B. Cross, C. Adamo, J. Jaramillo, R. Gomperts, R. E. Stratmann, O. Yazyev, A. J. Austin, R. Cammi, C. Pomelli, J. W. Ochterski, P. Y. Ayala, K. Morokuma, G. A. Voth, P. Salvador, J. J. Dannenberg, V. G. Zakrzewski, S. Dapprich, A. D. Daniels, M. C. Strain, O. Farkas, D. K. Malik, A. D. Rabuk, K. Raghavachari, J. B. Foresman, J. V. Ortiz, Q. Cui, A. G. Baboul, S. Clifford, J. Cioslowski, B. B. Stefanov, G. Liu, A. Liashenko, P. Piskorz, I. Komaromi, R. L. Martin, D. J. Fox, T. Keith, M. A. Al-Laham, C. Y. Peng, A. Nanayakkara, M. Challacombe, P. M. W. Gill, B. Johnson, W. Chen, M. W. Wong, C. Gonzalez, J. A. Pople, *Gaussian 2003*, Gaussian, Inc.: Pittsburgh, **2003**.
- [23] (a) R. Krishnan, J. S. Binkley, S. Seeger, J. A. Pople, *J. Chem. Phys.* **1980**, *72*, 650; (b) T. Clark, J. Chandrasekhar, G. W. Spitznagel, P. V. R. Schleyer, *J. Comput. Chem.* **1983**, *42*, 94.
- [24] P. Pulay, *Mol. Phys.* **1969**, *17*, 197.
- [25] (a) R. Ditchfield, *Mol. Phys.* **1974**, *27*, 789; (b) K. Wolinski, J. F. Hilton, P. Pulay, *J. Am. Chem. Soc.* **1990**, *112*, 8251.
- [26] A. D. Becke, *J. Chem. Phys.* **1993**, *98*, 5648.
- [27] C. Lee, W. Yang, R. P. Parr, *Phys. Rev.* **1988**, *B 38*, 785.
- [28] (a) D. E. Woon, T. H. Dunning, *J. Chem. Phys.* **1993**, *98*, 650; (b) R. A. Kendall, T. H. Dunning, R. J. Harrison, *J. Chem. Phys.* **1992**, *96*, 6796.
- [29] (a) J. E. Peralta, V. Barone, R. H. Contreras, D. G. Zaccari, J. P. Snyder, *J. Am. Chem. Soc.* **2001**, *123*, 9162; (b) V. Barone, J. E. Peralta, R. H. Contreras, D. G. Zaccari, J. P. Snyder *J. Am. Chem. Soc.* **2002**, *124*, 5607; (c) J. E. Peralta, G. E. Scuseria, J. R. Cheeseman, M. J. Frish, *Chem. Phys. Lett.* **2003**, *375*, 452.
- [30] E. D. Glendening, A. E. Reed, J. E. Carpenter, F. Weinhold, *Program as Implemented in the Gaussian 03*, NBO version 3.1, Revision D.02, Gaussian Inc.: Wallingford, **2004**.